Chapter 4

High-Order Approximation for Generalized Fractional Derivative and Its Application

In this chapter, the approximation of the generalized fractional derivative is studied. Numerical solutions of fractional advection-diffusion equation with this derivative are obtained. Section 4.1, provides some basic information about generalized fractional operator proposed in [33], which is briefly discussed in Chapter 1. In Section 4.2, the numerical scheme and stability is discussed. Section 4.3 presents numerical examples to support the numerical scheme, and compares the obtained results with the results given in [106]. Section 4.4 concludes the chapter.

4.1 Introduction

This chapter investigates a scheme using Taylor's expansion for generalized fractional Caputo derivative proposed by Agrawal in 2012 [33, 34] using scale and weight functions as key features. The theory of generalized fractional calculus was proposed by Kiryakova [197]. Erdélyi-Kober operator is widely used generalized fractional operator whose properties can be studied from [3, 197, 180]. Luchko and Trujillo [198] made Caputo modification to this operator. A brief survey on generalizations of fractional integrals and derivatives is given in [199]. The generalized multi-parameter operators proposed by Agrawal show that many integral and differential equations can be written and solved in an elegant way using these operators.

An advection-diffusion equation (ADE) is a combination of an advection equation and a diffusion equation, simulating transportation of mass or energy by the fluid in a movement. In this chapter, the generalized fractional advection-diffusion equation (GFADE) formed using generalized Caputo derivative in respect of time is being treated. The definitions used here are given in Chapter 1 (from Eq. (1.13)- Eq. (1.16)). The speciality of this definition is the presence of scale function and weight function, and by changing these functions, many important derivatives and integrals can be obtained, and hence many necessary equations can be studied simultaneously. The use of these generalized fractional derivatives and integrals in FADE makes it more attractive and useful over the other FADE. Such problems become complicated or sometimes impossible to solve analytically. So, it is necessary to know how to solve these equations numerically. Xu et al. [106] presented the numerical solution of GFADE by the finite difference method, where the order of scheme is estimated to one. This chapter develops a numerical method for GFADE with a higher order of convergence.

4.2 Main Result

The standard FADE is given by

$$\frac{\partial^\alpha u(x,t)}{\partial t^\alpha} + a(x,t)\frac{\partial u(x,t)}{\partial x} = v^2\frac{\partial^2 u(x,t)}{\partial x^2} + f(x,t), \tag{4.1}$$

where $\alpha \in (0,1)$, the real parameters $a(x,t)$ and $v > 0$ represent the average fluid velocity and dispersion coefficient, respectively, and $f(x,t)$ is the source term. Eq. (4.1) appears in describing solute transport in aquifers and u represents the solute concentration [13, 200]. FADEs describe transport at the earth surface. Since fractional derivatives are non-local, and hence FADEs, they model movement of fluid in influence of hydraulic conditions. FADEs with fractional derivative in time describe motion of particles with memory in time [14, 97].

In recent years, significant work has been done on the Eq. (4.1) when the fractional order derivative is considered as Caputo derivative. Many authors presented their perspectives to approximate Caputo derivative with a high order of convergence [69, 169, 164, 201, 202, 203]. Here, time fractional derivative is taken as generalized Caputo derivative and then Eq. (4.1) becomes GFADE:

$$\frac{{}^*\partial^\alpha u(x,t)}{{}^*\partial t^\alpha} + a(x,t)\frac{\partial u(x,t)}{\partial x} = v^2\frac{\partial^2 u(x,t)}{\partial x^2} + f(x,t), \tag{4.2}$$

where

$$\begin{aligned}\frac{{}^*\partial^\alpha u(x,t)}{{}^*\partial t^\alpha} &= {}_0^C D^\alpha_{t,(z,w)} u(x,t)\\ &= \frac{[w(t)]^{-1}}{\Gamma(1-\alpha)}\int_0^t \frac{1}{[z(t)-z(s)]^\alpha}\frac{\partial}{\partial s}[w(s)u(x,s)]ds.\end{aligned} \tag{4.3}$$

The Eq. (4.2) reduce to different FADEs for particular choices of scale and weight function. $z(t) = t$, and $w(t) = 1$ form Eq. (4.2) as an FADE with Caputo time-derivative, whereas $z(t) = \ln(t)$, and $w(t) = 1$, and $z(t) = t^{\sigma}$, and $w(t) = t^{\sigma\eta}$ gives FADE with Hadamard [204] and modified Erdélyi-Kober derivatives [205], respectively.

4.2.1 Formation of numerical scheme

For numerical solution of Eq. (4.2), consider the bounded domain $[0, b] \times [0, T]$, and the initial and boundary conditions as

$$u(x, 0) = u_0(x), \quad \forall\ x \in [0, b], \tag{4.4}$$

$$u(0, t) = g_1(t), \quad \text{and} \quad u(b, t) = g_2(t), \quad \forall\ t \geq 0. \tag{4.5}$$

Here, the method used for discretization is similar to the Method 2 in Chapter 2 (Subsection 2.2.2). Let $f(t)$ is a function whose fifth derivative is continuous and sixth derivative exists on the interval [0,T]. Let $0 = t_0 < t_1 < ... < t_n = T$, in which $t_k = k\tau$ where $\tau = \frac{T}{n}$. Recalling, the Taylor expansion for $f'(s)$ at $t = t_k$ for interval (t_k, t_{k+1}), $k = 0, 2, ..., n-1$ is given by

$$f'(s) = f'(t_k) + f''(t_k)(s - t_k) + \frac{f^{(3)}(t_k)}{2!}(s - t_k)^2 + O((s - t_k)^3),\ s \in (t_k, t_{k+1}). \tag{4.6}$$

Since,

$$f'(t_k) = \frac{f(t_{k+1}) - f(t_{k-1})}{2\tau} - \frac{f^{(3)}(t_k)}{3!}\tau^2 + O(\tau^4), \tag{4.7}$$

and,

$$f''(t_k) = \frac{f(t_{k+1}) - 2f(t_k) + f(t_{k-1})}{\tau^2} - \frac{f^{(4)}(t_k)}{12}\tau^2 + O(\tau^4), \tag{4.8}$$

hence,

$$f'(s) = \frac{f(t_{k+1}) - f(t_{k-1})}{2\tau} + \frac{f(t_{k+1}) - 2f(t_k) + f(t_{k-1})}{\tau^2}(s - t_k)$$

$$- \frac{f^{(3)}(t_k)}{3!}\tau^2 + \frac{f^{(3)}(t_k)}{2!}(s - t_k)^2 + O((s - t_k)^3),\ 0 < s - t_k < \tau. \tag{4.9}$$

So, generalized Caputo derivative can be discretized as

$$\frac{{}^*\partial^\alpha u(x_i, t_{j+1})}{{}^*\partial t^\alpha} = \frac{[w(t_{j+1})]^{-1}}{\Gamma(1-\alpha)} \int_0^{t_{j+1}} \frac{1}{[z(t_{j+1}) - z(s)]^\alpha} \frac{\partial}{\partial s}[w(s)u(x,s)]ds$$

$$= \frac{[w(t_{j+1})]^{-1}}{\Gamma(1-\alpha)} \sum_{k=0}^{j} \int_{t_k}^{t_{k+1}} \frac{1}{[z(t_{j+1}) - z(s)]^\alpha} \frac{\partial}{\partial s}[w(s)u(x,s)]ds, \tag{4.10}$$

where $x_i = x_0 + ih,\ i = 0, z1, 2, ..., m-1$, such that $0 = x_0 < x_1 < ... < x_m = b$, and $h = \frac{b}{m}$. Now, using symbol w_k for $w(t_k)$ and u_j^i for $u(x_i, t_j)$ for further calculations. Applying Eq. (4.9) to Eq. (4.10),

$$\frac{{}^*\partial^\alpha u(x_i,t_{j+1})}{{}^*\partial t^\alpha}$$

$$\approx \sum_{k=0}^{j} \{{}_1A_j^k(w_{k+1}u_{k+1}^i - w_{k-1}u_{k-1}^i) + {}_1B_j^k(w_{k+1}u_{k+1}^i - 2w_ku_k^i + w_{k-1}u_{k-1}^i)\}$$

$$= \sum_{k=0}^{j} \{(-\ {}_1A_j^k + \ {}_1B_j^k)w_{k-1}u_{k-1}^i + (-2_1B_j^k)w_k u_k^i + ({}_1A_j^k + \ {}_1B_j^k)w_{k+1}u_{k+1}^i\}$$

$$= \sum_{k=0}^{j} \{A_j^k u_{k-1}^i + B_j^k u_k^i + C_j^k u_{k+1}^i\}, \tag{4.11}$$

where

$${}_1A_j^k = \frac{[w(t_{j+1})]^{-1}}{\Gamma(1-\alpha)} \int_{t_k}^{t_{k+1}} \frac{[z(t_{j+1}) - z(s)]^{-\alpha}}{2\tau} ds, \tag{4.12}$$

$${}_1B_j^k = \frac{[w(t_{j+1})]^{-1}}{\Gamma(1-\alpha)} \int_{t_k}^{t_{k+1}} (s - t_k) \frac{[z(t_{j+1}) - z(s)]^{-\alpha}}{\tau^2} ds, \tag{4.13}$$

$$A_j^k = (-\ {}_1A_j^k + \ {}_1B_j^k)w_{k-1}, \tag{4.14}$$

$$B_j^k = (-2_1B_j^k)w_k, \tag{4.15}$$

$$C_j^k = ({}_1A_j^k + \ {}_1B_j^k)w_{k+1}. \tag{4.16}$$

Now, for solving ${}_1A_j^k$ and ${}_1B_j^k$, let $V = [z(t_{j+1}) - z(s)]$,

$$\begin{aligned} \Rightarrow dV &= -z'(s)ds \\ &= -\left(\frac{z(t_{k+1}) - z(t_k)}{\tau}\right) ds \text{ for } s \in (t_k, t_{k+1}), \end{aligned}$$

then

$$\int [z(t_{j+1}) - z(s)]^{-\alpha} ds = \frac{-\tau}{z(t_{k+1}) - z(t_k)} \frac{[z(t_{j+1}) - z(s)]^{1-\alpha}}{1-\alpha},$$

so

$$ {}_1A_j^k = \frac{[w(t_{j+1})]^{-1}}{\Gamma(3-\alpha)} \left\{ \frac{(2-\alpha)}{2} \frac{[z(t_{j+1}) - z(t_k)]^{1-\alpha} - [z(t_{j+1}) - z(t_{k+1})]^{1-\alpha}}{[z(t_{k+1}) - z(t_k)]} \right\}, \quad (4.17) $$

and

$$ {}_1B_j^k = \frac{[w(t_{j+1})]^{-1}}{\Gamma(3-\alpha)} \left\{ -(2-\alpha) \frac{[z(t_{j+1}) - z(t_{k+1})]^{1-\alpha}}{[z(t_{k+1}) - z(t_k)]} \right. $$

$$ \left. + \frac{[z(t_{j+1}) - z(t_k)]^{2-\alpha} - [z(t_{j+1}) - z(t_{k+1})]^{2-\alpha}}{[z(t_{k+1}) - z(t_k)]^2} \right\}. \quad (4.18) $$

Eq. (4.11) is the scheme for discretization of generalized fractional Caputo derivative of order α. In Section 4.3, it will be shown that the order of convergence of this scheme is $(3-\alpha)$ and $(2-\alpha)$ for the linear scale functions and non-linear scale functions, respectively.

Now, for approximating FADE, approximate the first and second order spatial derivative as follows

$$ \frac{\partial u(x_i, t_{j+1})}{\partial x} \approx \frac{u_{j+1}^i - u_{j+1}^{i-1}}{h}, \qquad i = 1, 2, ..., m-1, \quad (4.19) $$

$$ \frac{\partial^2 u(x_i, t_{j+1})}{\partial x^2} \approx \frac{u_{j+1}^{i+1} - 2u_{j+1}^i + u_{j+1}^{i-1}}{h^2}, \qquad i = 1, 2, ..., m-1. \quad (4.20) $$

Now, putting Eq. (4.19), Eq. (4.20), and Eq. (4.11) in Eq. (4.2),

$$ \sum_{k=0}^{j} \{A_j^k u_{k-1}^i + B_j^k u_k^i + C_j^k u_{k+1}^i\} + p_j^i (u_{j+1}^i - u_{j+1}^{i-1}) = q(u_{j+1}^{i+1} - 2u_{j+1}^i + u_{j+1}^{i-1}) + f_{j+1}^i, \quad (4.21) $$

where $p_j^i = \frac{a(x_i,t_{j+1})}{h}$, $q = \frac{v^2}{h^2}$, and $f_{j+1}^i = f(x_i, t_{j+1})$,

so

$$\sum_{k=0}^{j}\{A_j^k u_{k-1}^i + B_j^k u_k^i + C_j^k u_{k+1}^i\} + (-p_j^i - q)u_{j+1}^{i-1} + (p_j^i + 2q)u_{j+1}^i + (-q)u_{j+1}^{i+1} = f_{j+1}^i, \tag{4.22}$$

for $j = 0$,

$$(A_0^0 u_{-1}^i + B_0^0 u_0^i + C_0^0 u_1^i) + (-p_0^i - q)u_1^{i-1} + (p_0^i + 2q)u_1^i + (-q)u_1^{i+1} = f_1^i, \tag{4.23}$$

where $u_{-1}^i = u_0^i - \tau\frac{\partial u_0^i}{\partial t} + \frac{\tau^2}{2}\frac{\partial^2 u_0^i}{\partial t^2} + O(\tau^3)$. If $\frac{\partial u(x,0)}{\partial t} \neq 0$, the convergence order of scheme (4.22) is $O(\tau)$. So, here for higher convergence order, we consider the case when $\frac{\partial u(x,0)}{\partial t} = \frac{\partial^2 u(x,0)}{\partial t^2} = 0$, i.e. $u_{-1}^i = u_0^i$. Hence, arranging the Eq. (4.23)

$$(-p_0^i - q)u_1^{i-1} + (p_0^i + 2q + C_0^0)u_1^i + (-q)u_1^{i+1} = -(A_0^0 + B_0^0)u_0^i + f_1^i, \tag{4.24}$$

for $0 < j \leq m-1$,

$$(A_j^j u_{j-1}^i + B_j^j u_j^i + C_j^j u_{j+1}^i) + (-q - p_j^i)u_{j+1}^{i-1} + (p_j^i + 2q)u_{j+1}^i + (-q)u_{j+1}^{i+1}$$

$$= -\sum_{k=0}^{j-1}\{A_j^k u_{k-1}^i + B_j^k u_k^i + C_j^k u_{k+1}^i\} + f_{j+1}^i,$$

$$(-q - p_j^i)u_{j+1}^{i-1} + (p_j^i + 2q + C_j^j)u_{j+1}^i + (-q)u_{j+1}^{i+1}$$

$$= f_{j+1}^i - \sum_{k=0}^{j-1}\{A_j^k u_{k-1}^i + B_j^k u_k^i + C_j^k u_{k+1}^i\} - (A_j^j u_{j-1}^i + B_j^j u_j^i). \tag{4.25}$$

Lemma 4.2.1. Let the scale function $z(t) > 0$ is strictly monotone increasing, and the

weight function $w(t) > 0$ is monotone increasing, and $0 < \alpha < 1$ then the following results hold

(a) ${}_1A_j^k > 0$ and ${}_1B_j^k > 0$,

(b) ${}_1B_j^k >\ {}_1A_j^k$, and

(c) $A_j^k + B_j^k + C_j^k > 0$.

Proof. (a) Since

$${}_1A_j^k = \frac{[w(t_{j+1})]^{-1}}{\Gamma(3-\alpha)} \left\{ \frac{(2-\alpha)}{2} \frac{[z(t_{j+1}) - z(t_k)]^{1-\alpha} - [z(t_{j+1}) - z(t_{k+1})]^{1-\alpha}}{[z(t_{k+1}) - z(t_k)]} \right\},$$

and $z(t) > 0$ is strictly increasing function, so $z(t_{k+1}) > z(t_k)$, for $t_{k+1} > t_k$, which implies that $z(t_{k+1}) - z(t_k) > 0$, and $[z(t_{j+1}) - z(t_k)]^{1-\alpha} > [z(t_{j+1}) - z(t_{k+1})]^{1-\alpha}$ for $\alpha \in (0, 1)$. As $w(t) > 0$ is increasing function, so $w(t_{j+1}) > 0$ which shows that ${}_1A_j^k > 0$.

Now, for

$${}_1B_j^k = \frac{[w(t_{j+1})]^{-1}}{\Gamma(3-\alpha)} \left\{ -(2-\alpha) \frac{[z(t_{j+1}) - z(t_{k+1})]^{1-\alpha}}{[z(t_{k+1}) - z(t_k)]} \right.$$

$$\left. + \frac{[z(t_{j+1}) - z(t_k)]^{2-\alpha} - [z(t_{j+1}) - z(t_{k+1})]^{2-\alpha}}{[z(t_{k+1}) - z(t_k)]^2} \right\}.$$

$$[z(t_{j+1}) - z(t_{k+1})]^{2-\alpha} - [z(t_{j+1}) - z(t_k)]^{2-\alpha}$$

$$< [z(t_{j+1}) - z(t_{k+1})][z(t_{j+1}) - z(t_{k+1})]^{1-\alpha} - [z(t_{j+1}) - z(t_k)][z(t_{j+1}) - z(t_{k+1})]^{1-\alpha}$$

$$< (2-\alpha)[z(t_k) - z(t_{k+1})][z(t_{j+1}) - z(t_{k+1})]^{1-\alpha},$$

$$\Rightarrow \quad \frac{[z(t_{j+1}) - z(t_k)]^{2-\alpha} - [z(t_{j+1}) - z(t_{k+1})]^{2-\alpha}}{[z(t_{k+1}) - z(t_k)]^2} > (2-\alpha)\frac{[z(t_{j+1}) - z(t_{k+1})]^{1-\alpha}}{[z(t_{k+1}) - z(t_k)]},$$

which shows that ${}_1B_j^k > 0$.

(*b*) To show that ${}_1B_j^k > {}_1A_j^k$, i.e. ${}_1B_j^k - {}_1A_j^k > 0$,

i.e

$$-(2-\alpha)\frac{[z(t_{j+1}) - z(t_{k+1})]^{1-\alpha}}{[z(t_{k+1}) - z(t_k)]} + \frac{[z(t_{j+1}) - z(t_k)]^{2-\alpha} - [z(t_{j+1}) - z(t_{k+1})]^{2-\alpha}}{[z(t_{k+1}) - z(t_k)]^2}$$

$$-\frac{(2-\alpha)}{2}\ \frac{[z(t_{j+1}) - z(t_k)]^{1-\alpha} - [z(t_{j+1}) - z(t_{k+1})]^{1-\alpha}}{[z(t_{k+1}) - z(t_k)]} > 0,$$

i.e.

$$2\{[z(t_{j+1}) - z(t_k)]^{2-\alpha} - [z(t_{j+1}) - z(t_{k+1})]^{2-\alpha}\}$$

$$-(2-\alpha)[z(t_{k+1}) - z(t_k)]\{[z(t_{j+1}) - z(t_k)]^{1-\alpha} + [z(t_{j+1}) - z(t_{k+1})]^{1-\alpha}\} > 0,$$

i.e. to show that,

$$\alpha\{[z(t_{j+1}) - z(t_k)]^{2-\alpha} - [z(t_{j+1}) - z(t_{k+1})]^{2-\alpha}\}$$

$$-(2-\alpha)\{[z(t_{j+1}) - z(t_k)][z(t_{j+1}) - z(t_{k+1})]^{1-\alpha}$$

$$-[z(t_{j+1}) - z(t_{k+1})][z(t_{j+1}) - z(t_k)]^{1-\alpha}\} > 0. \tag{4.26}$$

Now, as

$$[z(t_{j+1}) - z(t_{k+1})]^{2-\alpha} - [z(t_{j+1}) - z(t_k)]^{2-\alpha}$$

$$< [z(t_{j+1}) - z(t_{k+1})][z(t_{j+1}) - z(t_k)]^{1-\alpha} - [z(t_{j+1}) - z(t_k)][z(t_{j+1}) - z(t_{k+1})]^{1-\alpha},$$

$$\Rightarrow \quad \alpha\{[z(t_{j+1}) - z(t_{k+1})]^{2-\alpha} - [z(t_{j+1}) - z(t_k)]^{2-\alpha}\}$$

$$< (2-\alpha)\left\{[z(t_{j+1}) - z(t_{k+1})][z(t_{j+1}) - z(t_k)]^{1-\alpha}\right.$$

$$\left. - [z(t_{j+1}) - z(t_k)][z(t_{j+1}) - z(t_{k+1})]^{1-\alpha}\right\},$$

$$\Rightarrow \quad \alpha\{[z(t_{j+1}) - z(t_k)]^{2-\alpha} - [z(t_{j+1}) - z(t_{k+1})]^{2-\alpha}\}$$

$$> (2-\alpha)\left\{[z(t_{j+1}) - z(t_k)][z(t_{j+1}) - z(t_{k+1})]^{1-\alpha}\right.$$

$$\left. - [z(t_{j+1}) - z(t_{k+1})][z(t_{j+1}) - z(t_k)]^{1-\alpha}\right\},$$

which proves Eq. (4.26), and hence (b).

(c)

$$A_j^k + B_j^k + C_j^k = (-{}_1A_j^k + {}_1B_j^k)w_{k-1} + (-2{}_1B_j^k)w_k + ({}_1A_j^k + {}_1B_j^k)w_{k+1}$$

$$= {}_1A_j^k(w_{k+1} - w_{k-1}) + {}_1B_j^k(w_{k-1} + w_{k-1} - 2w_k).$$

Since, from part (b), $\quad {}_1B_j^k > {}_1A_j^k, \quad$ so

$$A_j^k + B_j^k + C_j^k > {}_1A_j^k(2w_{k+1} - 2w_k) > 0.$$

□

4.2.2 Stability of the numerical scheme

Theorem 4.2.1. (Lax-Richtmyer Theorem, [206]) For consistent numerical methods to approximate the solution of a well-posed linear differential equation, stability and convergence are equivalent.

So, it is sufficient to show that the scheme (4.22) is stable for the convergence of the numerical scheme.

Theorem 4.2.2. Let $z(t)$ be positive and strictly increasing function, and $w(t)$ be positive and increasing function, then the above scheme for solving GFADE is stable.

Proof. For stability of the above inhomogeneous scheme, it suffices to show that the corresponding homogeneous scheme is stable.
So, let the solution of the Eq. (4.2) be of the form $u_j^l = \xi_j e^{iwly}$, $i = \sqrt{-1}$. w is real number, and $1 \leq l \leq m-1$. Hence, from Eq. (4.22),

$$(-q - p_j^l)e^{iw(l-1)y} + (p_j^l + 2q + C_j^j)\xi_{j+1}e^{iwly} + (-q)\xi_{j+1}e^{iw(l+1)y}$$

$$= -\sum_{k=0}^{j-1}\{A_j^k\xi_{k-1}e^{iwly} + B_j^k\xi_k e^{iwly} + C_j^k\xi_{k+1}e^{iwly}\} - (A_j^j\xi_{j-1}e^{iwly} + B_j^j\xi_j e^{iwly}),$$

$$\Rightarrow \quad [(-q-p_j^l)e^{-iwy}+(p_j^l+2q+C_j^j)+(-q)e^{iwy}]\xi_{j+1}$$

$$=-\sum_{k=0}^{j-1}\{A_j^k\xi_{k-1}+B_j^k\xi_k+C_j^k\xi_{k+1}\}-(A_j^j\xi_{j-1}+B_j^j\xi_j),$$

$$\Rightarrow \quad [2q(1-\cos wy)+p_j^l(1-e^{-iwy})+C_j^j]\xi_{j+1}$$

$$=-\sum_{k=0}^{j-1}\{A_j^k\xi_{k-1}+B_j^k\xi_k+C_j^k\xi_{k+1}\}-(A_j^j\xi_{j-1}+B_j^j\xi_j),$$

since, $p_j^l(1-e^{-iwy})\geq 0$, so

$$[2q(1-\cos wy)+C_j^j]\xi_{j+1}\leq -\sum_{k=0}^{j-1}\{A_j^k\xi_{k-1}+B_j^k\xi_k+C_j^k\xi_{k+1}\}-(A_j^j\xi_{j-1}+B_j^j\xi_j).$$

According to Lemma (4.2.1), $(A_j^k+B_j^k+C_j^k)$ is positive, so

$$[2q(1-\cos wy)+C_j^j]\xi_{j+1}\leq -(A_j^j\xi_{j-1}+B_j^j\xi_j),$$

$$\Rightarrow \quad \xi_{j+1}\leq \frac{(-A_j^j)\xi_{j-1}+(-B_j^j)\xi_j}{[2q(1-\cos wy)+C_j^j]},$$

$$\xi_{j+1}\leq \frac{(-A_j^j)\xi_{j-1}+(-B_j^j)\xi_j+(-C_j^j)\xi_j}{[2q(1-\cos wy)+C_j^j]}+\frac{C_j^j}{[2q(1-\cos wy)+C_j^j]}\xi_j,$$

$$\xi_{j+1}\leq \xi_j,$$

since, $(A_j^j+B_j^j+C_j^j)$ is positive, and $C_j^j\leq 2q(1-\cos wy)+C_j^j$. This implies that $\xi_{j+1}\leq\xi_j\leq\cdots\leq\xi_1\leq\xi_0=|u_0|$, which shows that the scheme (4.22) is stable. The

consistency of the numerical scheme (4.22) can easily be verified, so Lax-Richtmyer Theorem clears that the numerical scheme (4.22) is convergent. □

4.3 Numerical Examples

This section presents some numerical results which verify the stability of the scheme. First, to calculate the order of convergence of our scheme, then compare that of the method given in [106]. The first example shows the stability and convergence of the scheme defined in Eq. (4.11) for approximating generalized fractional Caputo derivative, the second example verifies the same for the approximation of a GFADE, and the third example studies the effects of scale functions and weight functions on the solution of a GFADE.

Example 4.3.1. Consider the function $f(t) = t^4$.

Table 4.1 shows maximum absolute errors (MAE) and order of convergence (CO) obtained in the calculation of generalized fractional Caputo derivative of function $f(t) = t^4$ with the help of scheme 4.11, when $z(t) = t$ and $w(t) = 1$ for $\alpha = 0.2,\ 0.6,$ and 0.8. Table 4.2 represents the data of MAE and CO, when $w(t)$ changes while $z(t) = t$ is fixed. Take $w(t) = t + 1$ and e^t as linear function and non-linear function, respectively. In both cases, the scheme gives $(3 - \alpha)$ order of convergence. In Table 4.3, take $z(t)$ as a non-linear function $t^{1/2}$. In this case, the scheme gives $(2 - \alpha)$ order of convergence.

Example 4.3.2. Consider the following GFADE:

$$\frac{{}^{*}\partial^{\alpha}u(x,t)}{{}^{*}\partial t^{\alpha}} + a(x,t)\frac{\partial u(x,t)}{\partial x} = v^2\frac{\partial^2 u(x,t)}{\partial x^2} + f(x,t),\ 0 < t < 1,\ 0 < x < 1, \quad (4.27)$$

TABLE 4.1: MAE and CO of Example 4.3.1 with $z(t) = t$, and $w(t) = 1$ for different values of α.

Δt	$\alpha = 0.2$		$\alpha = 0.6$		$\alpha = 0.8$	
	MAE	CO	MAE	CO	MAE	CO
1/20	0.00024094		0.00278679		0.00753897	
1/40	3.7575E-05	2.68083	0.00054517	2.35382	0.00167938	2.16644
1/80	5.7436E-06	2.70976	0.00010520	2.37361	0.00036991	2.18270
1/160	8.6640E-07	2.72885	2.01464E-05	2.38450	8.1011E-05	2.19097
1/320	1.2948E-07	2.74233	3.84174E-06	2.39069	1.7689E-05	2.19524

TABLE 4.2: MAE and CO of Example 4.3.1 with $z(t) = t$, and $w(t) = e^t,\ t + 1$ for different values of α.

Δt	$\alpha = 0.2,\ w(t) = e^t$		$\alpha = 0.6,\ w(t) = t + 1$		$\alpha = 0.8,\ w(t) = t + 1$	
	MAE	CO	MAE	CO	MAE	CO
1/20	0.00063502		0.00470326		0.01280025	
1/40	0.00010336	2.61912	0.00093491	2.33077	0.00289327	2.14540
1/80	1.6216E-05	2.67218	0.00018197	2.36109	0.00064208	2.171876
1/160	2.4876E-06	2.70457	3.5018E-05	2.37755	0.00014117	2.185366
1/320	3.7608E-07	2.72567	6.6960E-06	2.38674	3.0887E-05	2.192327

with $u(x, 0) = \sin(2\pi x)$, and $u(0, t) = u(1, t) = 0$, where $a(x, t) = 10^{-6},\ v = 1$, and $f(x, t) = \frac{2}{\Gamma(3-\alpha)}(x^2 - x)t^{2-\alpha} + 10^{-6}[2\pi\cos(2x\pi) + (2x - 1)t^2] + 4\pi^2\sin(2\pi x) - 2t^2$.

Let $z(t) = t$, and $w(t) = 1$, then the exact solution of Eq. (4.27) is $U(x, t) = \sin(2\pi x) + x(x - 1)t^2$. Solve Eq. (4.27) by the numerical scheme with step size $\triangle x = \triangle t = 0.001$ for different values of α. The numerical solutions and the exact solution are plotted in Figure 4.1. It is clear from the figure that the numerical

TABLE 4.3: MAE and CO of Example 4.3.1 with $z(t) = t^{1/2}$, and $w(t) = 1$ for different values of α.

Δt	$\alpha = 0.2$		$\alpha = 0.6$,		$\alpha = 0.8$	
	MAE	CO	MAE	CO	MAE	CO
1/20	0.00109416		0.01612312		0.04887215	
1/40	0.00029749	1.87889	0.00543670	1.56833	0.01860075	1.39365
1/80	8.4667E-05	1.81299	0.00193278	1.49205	0.00749705	1.31097
1/160	2.4693E-05	1.77772	0.00070937	1.44608	0.00313186	1.25930
1/320	7.2763E-06	1.76281	0.00026483	1.42147	0.0013348	1.23043

solutions agree with the exact one. Furthermore, on solving Eq. (4.27) with different step sizes, the MAE and CO can be calculated, and for this example, the results are given in Table 4.4 and Table 4.5. Also, in Table 4.4, the order of convergence of the numerical scheme described in [106] is given. These comparisons directly clarify that the scheme (4.22) is of a higher order of convergence. In Table 4.6, MAE and CO are shown when space step size Δx is fixed to 0.001, and in Table 4.7, the same is done when the time step size Δt is fixed to 0.002.

Example 4.3.3. Consider the GFADE (4.27) with $u(x,0) = u(0,t) = u(1,t) = 0$, and $a(x,t) = 0,\ v = 1$, and $f(x,t) = \frac{120}{\Gamma(6-\alpha)} t^{5-\alpha} e^{-t} \sin(\pi x) + \pi^2 t^5 e^{-t} \sin(\pi x)$.

In case of $z(t) = t$, and $w(t) = e^t$, the exact solution will be $U(x,t) = t^5 e^{-t} \sin(\pi x)$. The exact solution and the numerical solutions for different values of α are displayed in Figure 4.2 when the step sizes are $\Delta x = \Delta t = 0.002$. Table for MAE and CO at different step sizes for $\alpha = 0.9,\ 0.6$ and, 0.45 is given in Table 4.8. Table 4.9, and Table 4.10 show the MAE and CO, when the space step size Δx is fixed to 0.001, and the time step size Δt is fixed to 0.002, respectively.

TABLE 4.4: MAE and CO of Example 4.3.2 with different step-sizes Δt and Δx for $\alpha = 0.95$.

Δt	Δx	Absolutly Error	CO	CO [106]
1/8	1/8	0.05379458		
1/16	1/16	0.013118117	2.035900	1.3648
1/32	1/32	0.003224397	2.024459	1.1948
1/64	1/64	8.024769E-04	2.006498	1.0753
1/128	1/128	2.005455E-04	2.000531	1.0199
1/256	1/256	5.013081E-05	2.000160	1.0026
1/512	1/512	1.2531862E-05	2.000097	0.9986
1/1024	1/1024	3.1327208E-06	2.000112	0.9979

TABLE 4.5: MAE and CO of Example 4.3.2 with different step-sizes Δt and Δx for $\alpha = 0.6$ and 0.45.

Δt	Δx	$\alpha = 0.6$			$\alpha = 0.45$		
		MAE	CO	Time(s)	MAE	CO	Time(s)
1/8	1/8	0.05236263		0.025	0.05213485		0.026
1/16	1/16	0.01279691	2.032742	0.074	0.01274335	2.032503	0.072
1/32	1/32	0.00318142	2.008052	0.273	0.00316824	2.007992	0.276
1/64	1/64	0.00079426	2.001981	1.089	0.00079098	2.001965	1.087
1/128	1/128	0.00019850	2.000492	4.311	0.00019768	2.000487	4.312
1/256	1/256	4.9620E-05	2.000142	17.63	4.9415E-05	2.000129	17.49
1/512	1/512	1.2404E-05	2.000067	73.38	1.2353E-05	2.000067	73.02
1/1024	1/1024	3.1009E-06	2.000095	325.5	3.0881E-06	2.000096	325.8

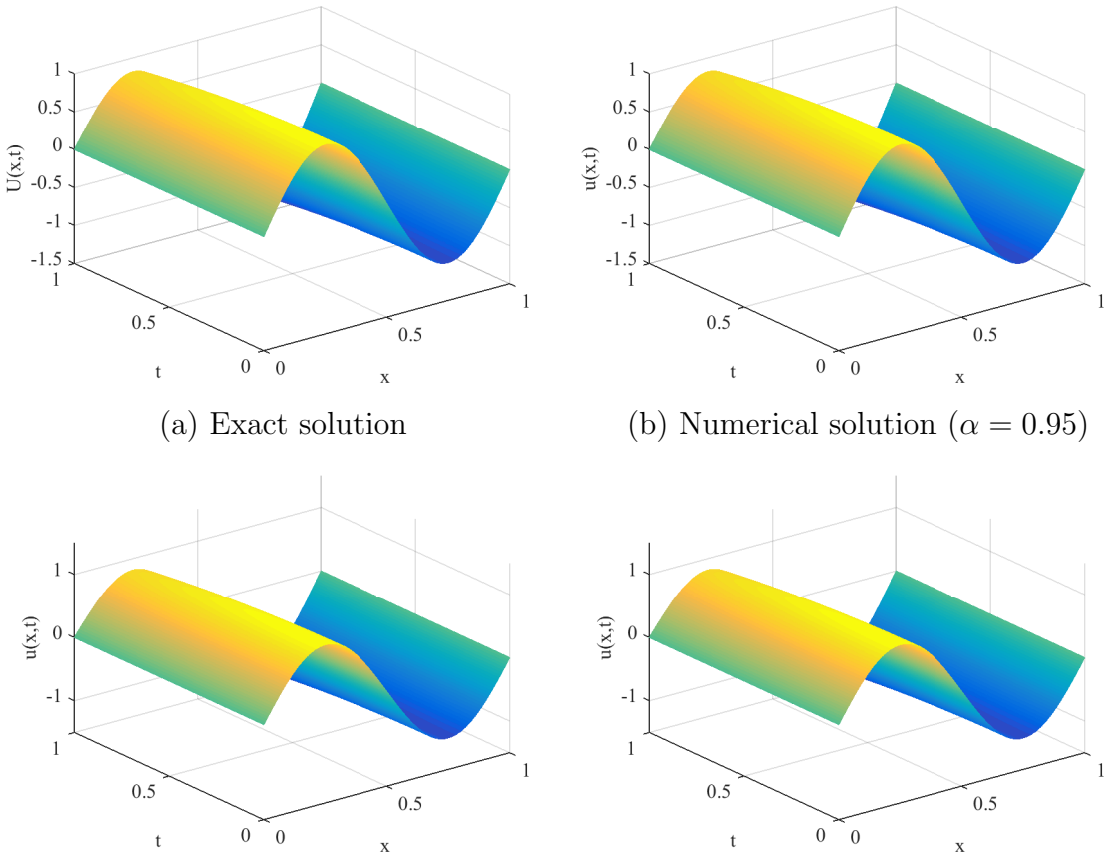

(a) Exact solution

(b) Numerical solution ($\alpha = 0.95$)

(c) Numerical solution ($\alpha = 0.6$)

(d) Numerical solution ($\alpha = 0.45$)

FIGURE 4.1: Comparison of the exact and the numerical solutions of Example 4.3.2.

TABLE 4.6: MAE and CO of Example 4.3.2 with different Δt, fixing $\Delta x = 0.001$ for different values of α.

Δt	$\alpha = 0.2$		$\alpha = 0.6$		$\alpha = 0.8$	
	MAE	CO	MAE	CO	MAE	CO
1/8	0.00065020		0.00023049		0.00012711	
1/16	0.00021085	1.62470	7.4915E-05	1.62137	4.0156E-05	1.66239
1/32	6.5164E-05	1.69405	2.3782E-05	1.65538	1.3292E-05	1.59505
1/64	2.0169E-05	1.69193	8.0738E-06	1.55855	5.5579E-06	1.25796

TABLE 4.7: MAE and CO of Example 4.3.2 with different Δx, fixing $\Delta t = 0.002$ for different values of α.

Δx	$\alpha = 0.95$		$\alpha = 0.6$		$\alpha = 0.45$	
	MAE	CO	MAE	CO	MAE	CO
1/8	0.05295249		0.05238486		0.05215782	
1/16	0.01293273	2.03367	0.01279940	2.03307	0.01274597	2.03284
1/32	0.00321453	2.00835	0.00318170	2.00820	0.00316855	2.00815
1/64	0.00080247	2.00209	0.00079430	2.00205	0.00079102	2.00204

TABLE 4.8: MAE and CO of Example 4.3.3 with different step-sizes Δt and Δx for $\alpha = 0.9, 0.6$, and 0.45.

Δt	Δx	$\alpha = 0.9$		$\alpha = 0.6$		$\alpha = 0.45$	
		MAE	CO	MAE	CO	MAE	CO
1/8	1/8	0.00871351		0.00538041		0.00474765	
1/16	1/16	0.00221356	1.97688	0.00127876	2.07297	0.00113616	2.06309
1/32	1/32	0.00054693	2.01695	0.00030263	2.07912	0.00027316	2.05629
1/64	1/64	0.00013312	2.03865	7.1845E-05	2.07459	6.6151E-05	2.04595
1/128	1/128	3.2162E-05	2.04927	1.7171E-05	2.06492	1.6139E-05	2.03522
1/256	1/256	7.7458E-06	2.05387	4.1353E-06	2.05391	3.9628E-06	2.02594
1/512	1/512	1.8636E-06	2.05534	1.0031E-06	2.04350	9.7799E-07	2.01863
1/1024	1/1024	4.4840E-07	2.05522	2.4486E-07	2.03445	2.4228E-07	2.013132

Table 4.11 provides executing time in seconds taken by the MATLAB program to calculate MAE for Example 4.3.2 and Example 4.3.3 at different step sizes and for different values of α.

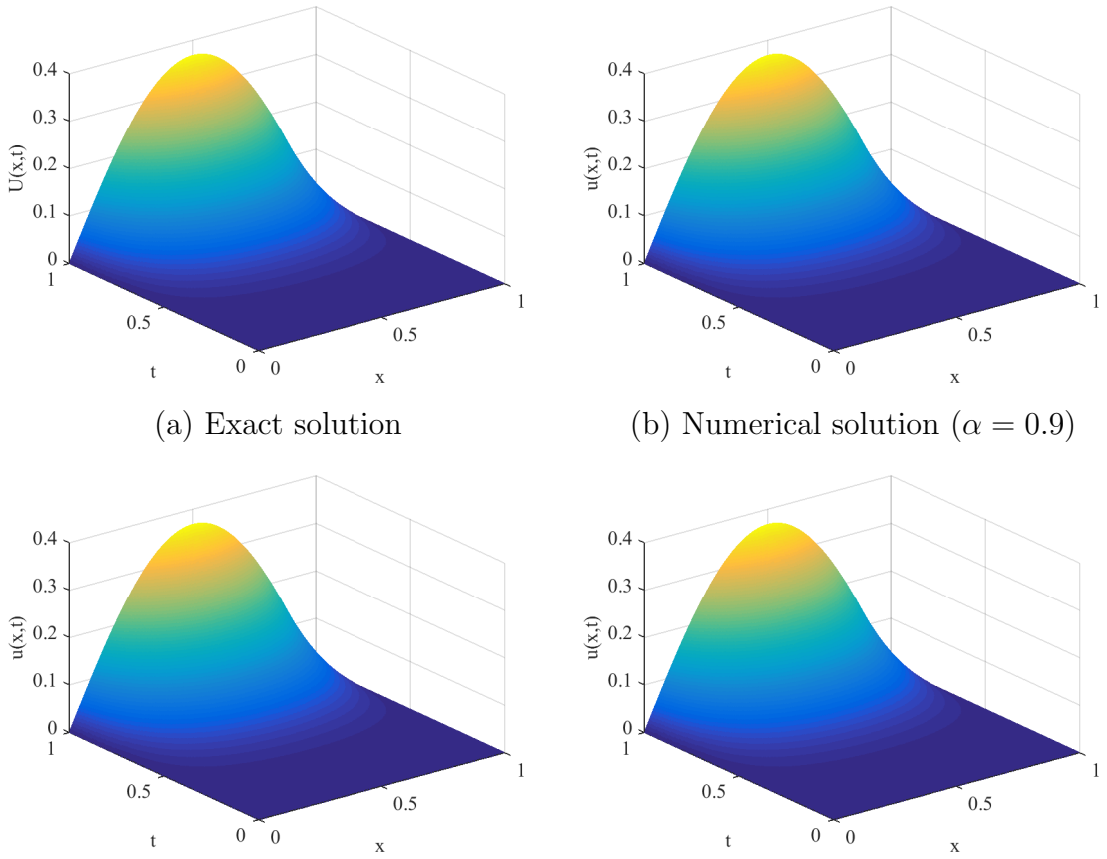

(a) Exact solution (b) Numerical solution ($\alpha = 0.9$)

(c) Numerical solution ($\alpha = 0.6$) (d) Numerical solution ($\alpha = 0.45$)

FIGURE 4.2: Comparison of the exact and the numerical solutions of Example 4.3.3.

TABLE 4.9: MAE and CO of Example 4.3.3 with different Δt, fixing $\Delta x = 0.001$ for different values of α.

Δt	$\alpha = 0.95$		$\alpha = 0.6$		$\alpha = 0.45$	
	MAE	CO	MAE	CO	MAE	CO
1/8	0.00534853		0.00162414		0.00081970	
1/16	0.00139518	1.93869	0.00035027	2.21312	0.00016199	2.33925
1/32	0.00034399	2.02001	7.1279E-05	2.29693	3.0246E-05	2.42106
1/64	8.2632E-05	2.05759	1.4218E-05	2.32575	5.6319E-06	2.42503

TABLE 4.10: MAE and CO of Example 4.3.3 with different Δx, fixing $\Delta t = 0.002$ for different values of α.

Δx	$\alpha = 0.95$		$\alpha = 0.6$		$\alpha = 0.45$	
	MAE	CO	MAE	CO	MAE	CO
1/8	0.00325498		0.00372096		0.00390985	
1/16	0.00081244	2.00231	0.00092691	2.00517	0.00097352	2.00583
1/32	0.00020382	1.99496	0.00023160	2.00083	0.00024316	2.00133
1/64	5.1792E-05	1.97651	5.7964E-05	1.99837	6.0796E-05	1.99983

TABLE 4.11: CPU time (seconds) in calculating MAE for Example 4.3.2 and Example 4.3.3 at different step sizes.

Δx	Δt	Time (Example 4.3.2)			Time (Example 4.3.3)		
		$\alpha = 0.6$	$\alpha = 0.45$	$\alpha = 0.9$	$\alpha = 0.6$	$\alpha = 0.45$	$\alpha = 0.9$
1/20	1/20	0.0118	0.0119	0.0118	0.0122	0.0120	0.0120
1/40	1/40	0.0333	0.0332	0.0333	0.0360	0.0356	0.0354
1/200	1/200	0.9434	0.1466	0.1464	0.1759	0.1795	0.1770
1/500	1/500	2.6895	2.7154	2.6970	2.7647	2.7958	2.7915
1/1000	1/1000	25.123	25.270	25.160	26.391	26.505	26.700

4.3.1 Effect of scale and weight functions on the solution

Example 4.3.4. Consider the GFADE (4.27) with $u(x,0) = x(1-x)\sin(4\pi x)$, and $u(0,t) = u(1,t) = 0$, where $v = 1.5$, $f(x,t) = \exp(-x - t^2)$, and $\alpha = 0.9$.

This example is considered to observe the effects of advection coefficient on the solution of FADE. Draw the graph of numerical solutions of Example 4.3.4 by taking $a(x,t) = x^4 + t^3$, and $50(x^4 + t^3)$ at step sizes $\Delta t = \Delta x = 0.005$ which is shown

in Figure 4.3. It is clear from the figure that if the amplitude of the advection coefficient is increased, then there is also an increment in the diffusion rate.

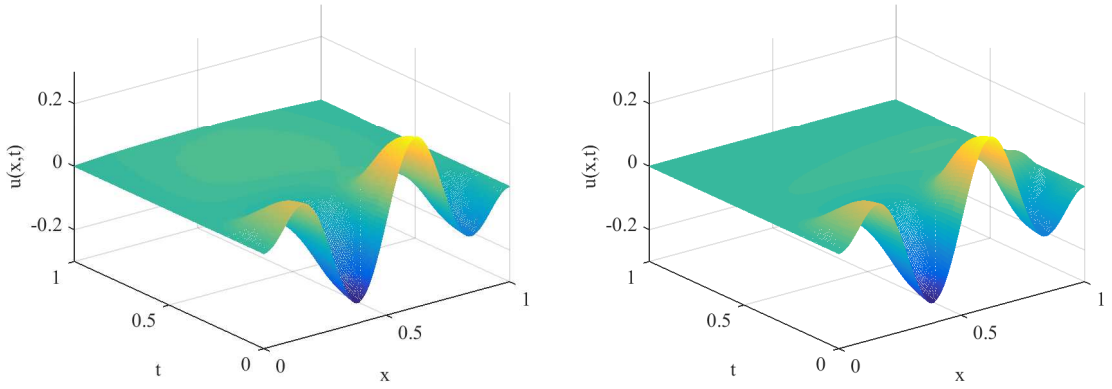

(a) $a(x,t) = x^4 + t^3$ (b) $a(x,t) = 100(x^4 + t^3)$

FIGURE 4.3: The numerical solutions of Example 4.3.4 with different advection coefficient $a(x,t)$.

Example 4.3.5. Consider the GFADE (4.27) with $u(x,0) = \sin(2\pi x)$, and $u(0,t) = u(1,t) = 0$, where $a(x,t) = \tan(t + e^x)$, $v = \frac{59}{3}\pi$, and $f(x,t) = 0$.

To see the effect of α, $w(t)$, and $z(t)$ on the diffusion governed by Eq. (4.27) with the above details at step-sizes $\Delta t = \Delta x = 0.01$, firstly, fix $z(t) = \exp(t^4/8)$, and $w(t) = \pi + \sin(\pi t)$, and vary α as 0.3, 0.4, 0.6, and 0.8. It is observed from Figure 4.4 that with the increment in the value of α, the rate of diffusion becomes slow. This implies that the diffusion process is inversely proportional to the fractional order.

When $\alpha = 0.9$ and $z(t) = \exp(t^4/8)$ are fixed, and weight function changes as $\exp(t)$, $\exp(2t)$, $\exp(4t)$, and $\exp(6t)$, then it can be observed from Figure 4.5 that the increment in weight function makes the process decay faster which implies that the diffusion is directly affected by the weight function.

Now, $\alpha = 0.9$ and $w(t) = \pi + \sin(\pi t)$ are fixed, and $z(t) = 0.005t,\ 0.05t$ are taken as linear scale functions, and $z(t) = t^2,\ t^4$ as non-linear scale functions. Here, linear scale functions are chosen to be contracting functions. The observations from Figure

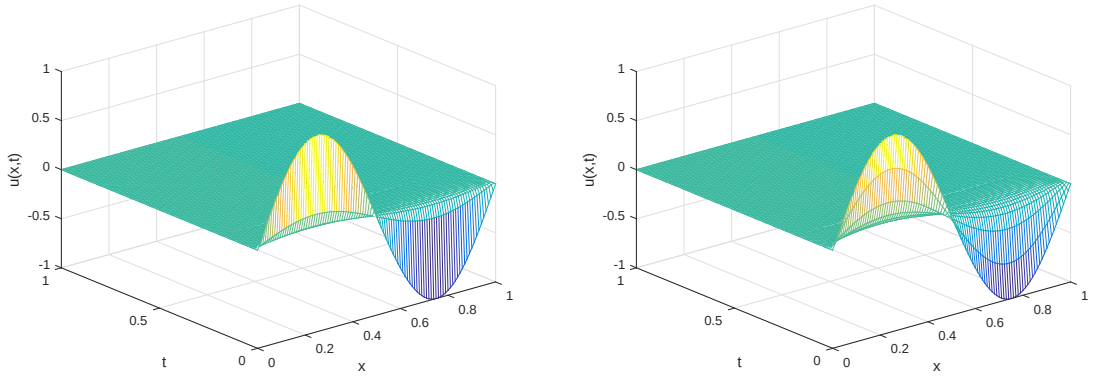

(a) $\alpha = 0.3$ (b) $\alpha = 0.4$

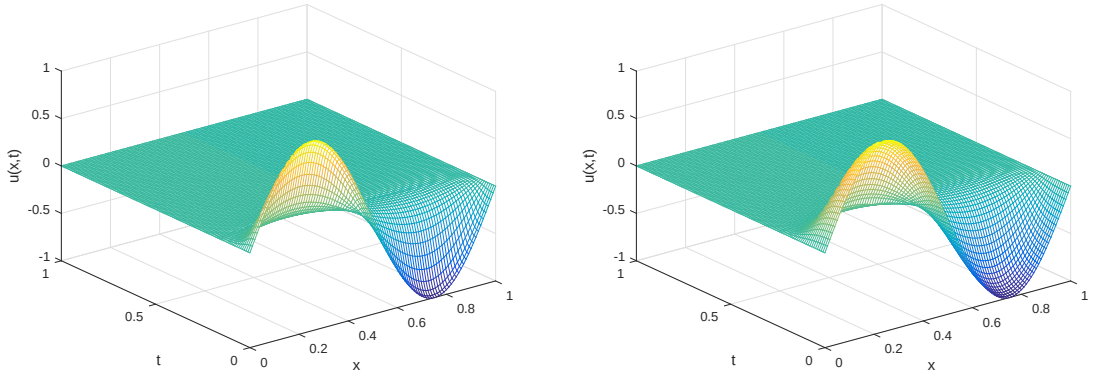

(c) $\alpha = 0.6$ (d) $\alpha = 0.8$

FIGURE 4.4: The numerical solutions of Example 4.3.5 with different values of α.

4.6 (a) and Figure 4.6 (b) are that if the scale function increases, the decay process becomes faster, i.e. in case of linear scale function, contraction makes the diffusion process slow. In case of non-linear scale functions, increasing function makes the process decay faster, see Figure 4.6(c) and Figure 4.6 (d).

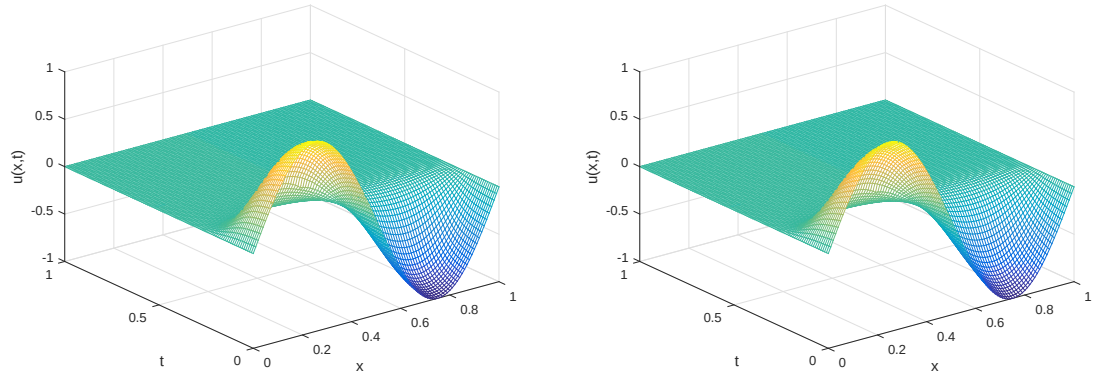

(a) $w(t) = \exp(t)$

(b) $w(t) = \exp(2t)$

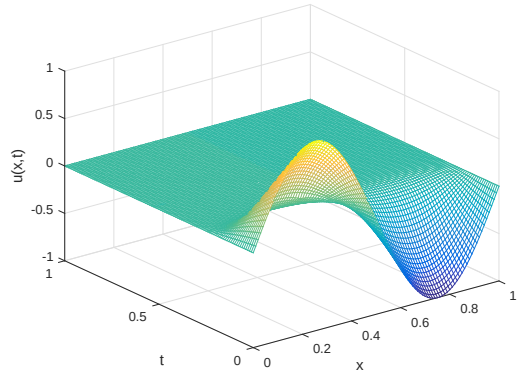

(c) $w(t) = \exp(4t)$

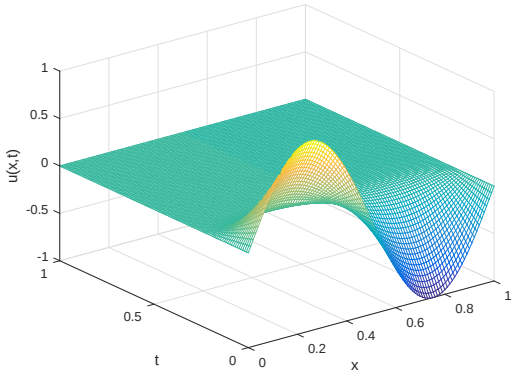

(d) $w(t) = \exp(6t)$

FIGURE 4.5: The numerical solutions of Example 4.3.5 with different weight functions.

4.4 Conclusion

In this paper, the Taylor series expansion is used to approximate generalized fractional derivative of Caputo type of order $\alpha \in (0, 1)$. This approximation helped to develop the numerical scheme for GFADE, which shows higher order of convergence when compared to Xu's paper. The generalized fractional time-derivative contains scale function and weight function, which changes the domain as desired and makes model flexible. There are still many problems in the physical world that are unsolved due to their complexity, and with the help of the proposed numerical scheme of a higher order, their numerical solutions can be calculated with good precision. The

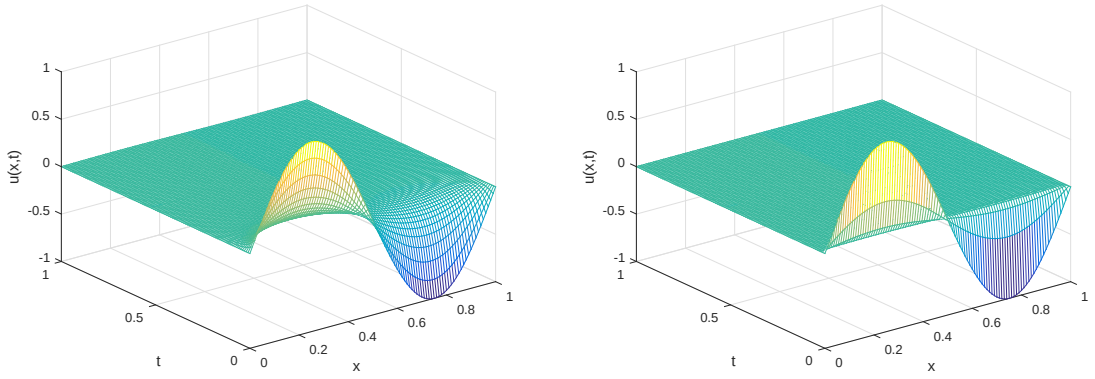

(a) $z(t) = 0.005t$ (b) $z(t) = 0.05t$

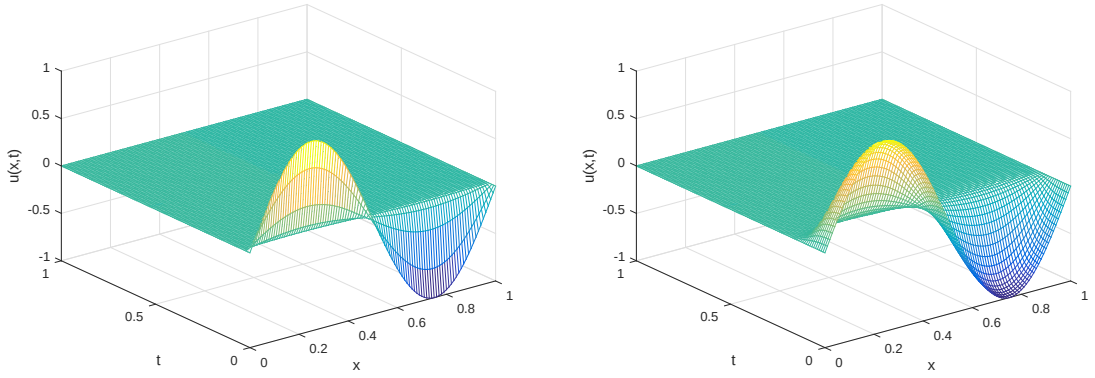

(c) $z(t) = t^2$ (d) $z(t) = t^4$

FIGURE 4.6: The numerical solutions of Example 4.3.5 with different scale functions.

stability of the numerical scheme is proved by Von Neumann analysis, and numerical examples are given to support the statements. Some examples are there to show the effect of α, $z(t)$, and $w(t)$ on the diffusion process of the equations.

The order of convergence, somehow, depends on the functions $z(t)$, $w(t)$, and fraction order α, which is yet to be discussed. Such studies will be presented in the near future.